Comparing Measurements, [7]Be Radiotracer Technique and Process-Based Erosion Model for Estimating Short-term Soil Loss from Cultivated Land in Northern Germany

Detlef DEUMLICH [1]*, Abhinand JHA [2] and Gerald KIRCHNER [3]

[1]Leibniz-Zentrum für Agrarlandschaftsforschung (ZALF), Müncheberg, Germany; [2]Bundesamt für Strahlenschutz, Salzgitter, Germany; [3]University of Hamburg/ZNF, Hamburg, Germany
*Corresponding author: ddeumlich@zalf.de

Abstract

Deumlich D., Jha A., Kirchner G. (2017): Comparing measurements, [7]Be radiotracer technique and process-based erosion model for estimating short-term soil loss from cultivated land in Northern Germany. Soil & Water Res., 12: 177–186.

Due to changing climate and irregular weather patterns, event-based soil loss and sediment yield have become important issues in the agricultural areas. Several mathematical models and prediction methodologies have been used to estimate event-based soil loss and soil redistribution based on soil types, land management, hydrology and local topography. The use of short-lived beryllium-7 as a means of estimating event-based soil erosion/deposition rates has become an alternative to the traditional soil loss measurement methods. A new erosion model taking into account the movement of [7]Be in soils has been presented recently. In order to direct the attention to the potential offered by this technique (measurements and mathematical model), a two-year study was performed at the erosion plots in Müncheberg, Germany, and twelve individual erosion rates were estimated. This paper presents a systematic comparison of the non-steady state [7]Be model with the process-based erosion model EROSION-3D and measured data. The results demonstrate a close consistency between the erosion rates estimated by erosion models and the estimates provided by the [7]Be model and can therefore be seen as a promising contribution to validating the use of this radionuclide to document short-term soil redistribution within the plot and deposited sediment at the bottom of the plot.

Keywords: beryllium-7; EROSION-3D; fallout radionuclides; sediment; water erosion

Accelerated soil erosion has troubled mankind ever since agriculture has been practiced and the literature lists its numerous gloomy and catastrophic effects. Total land area worldwide affected by water erosion is 1094 million ha, of which 749 million ha are severely affected, and that under wind erosion is 548 million ha, of which 280 million ha are severely affected (Oldeman 1994).

Soil erosion by water as investigated and discussed here is a complex time-variant process. It is a three-phase process with the detachment of individual particles from soil mass as the first phase followed by their transport by erosive agents such as water as the second phase. When sufficient energy is not available, the third phase of particle deposition occurs (Hjulström 1935; Young & Onstad 1976). Tillage plays an important role of translocation, which leads to the transport of soil downslope (Govers *et al.* 1996; Sommer *et al.* 2008). During the early stages of a heavy rainfall event, processes that occur in the field include surface and splash erosion. As the event proceeds, the flow frequently becomes concentrated, and rills are developed. Sediment that is detached from the interrill areas moves laterally to the rills in the thin interrill sheet flow (Meyer *et al.* 1975). Direct splash to the rills or downslope is not a major mode of transport (Malam Issa *et al.* 2006).

The fallout radionuclide ^{137}Cs is used widely for obtaining quantitative information on soil erosion and sediment redistribution rates within agricultural

landscapes, over several spatial and temporal scales, and it is frequently seen to represent a valuable complement to conventional soil erosion measurement techniques (Ritchie & Ritchie 2007; Walling & Bradley 1988; Walling & Woodward 1992; Wallbrink & Murray 1993; Walling & Quine 1995; Walling *et al*. 1999; Zapata 2002, 2003, 2007; Matisoff *et al*. 2002; Schuller *et al*. 2004; Porto & Walling 2014). However, measurements of this radionuclide provide estimates of medium-term (i.e. 40–50 years) soil erosion rates. The shorter-term perspective provided by the ^{7}Be method has the potential to estimate soil erosion rates associated with individual events or short periods. The ^{7}Be method has become increasingly relevant in an environment impacted by climate change, changing land use and other human activities.

Beryllium-7 is a short-lived cosmogenic radionuclide, produced in the upper atmosphere by spallation, which is deposited on the earth's surface by wet and dry fallout (Olsen *et al*. 1985; Rosner *et al*. 1996; Rodenas *et al*. 1997). Its half-life is 53.22 ± 0.06 days (Tilley *et al*. 2002) and it is easily detected by gamma spectrometry using its 477.6 keV photopeak.

Field and laboratory experiments performed since the early 1990s indicate that ^{7}Be in bare soils as well as in soils covered with vegetation often shows an approximately exponential decrease with depth, with most of the activity found within the upper few millimetres of the soil surface (Walling & Woodward 1992; Wallbrink & Murray 1996; Walling *et al*. 1999; Schuller *et al*. 2006, 2008). An exponential decline of ^{7}Be with depth indicates equilibrium between deposition and decay. Assuming exponential depth profiles, the ^{7}Be technique was applied for estimating soil erosion and deposition processes associated with individual periods of heavy rain at scales ranging from

plots of a few square meters to fields of a few hectares (Blake *et al*. 1999; Walling *et al*. 1999; Wilson *et al*. 2003; Schuller *et al*. 2006, 2008; Porto & Walling 2014). An approach to estimating erosion/deposition rates if ^{7}Be inventories are not in equilibrium (e.g. after ploughing or multiple erosion events within a few weeks) has been developed recently (Jha *et al*. 2015) and applied successfully.

The aim of this paper is to compare the performance of the non-steady state transport model of ^{7}Be presented in our previous paper (Jha *et al*. 2015) with a process based erosion model, EROSION-3D.

MATERIAL AND METHODS

Study site. The experimental field (Figure 1) is situated at Müncheberg, Germany (52.6°N, 14.3°E). The measurement plot is conventionally ploughed up to a depth of 25 cm in June and October. Sorghum (*Sorghum sudanense*) is grown during summer months followed by winter rye (*Secale cereale*) every year. Eroded soil and runoff were concentrated and collected in a sampler system (Figure 1). Rainfall data were obtained from an automatic weather station to characterise the storm events based on the R-factor of USLE (Wischmeier & Smith 1978, DIN 19708: 2005). The texture is light silty sand (German classification: Su2 with 3% clay, 16% silt, 81% sand; AG Boden 2005), C_{org} is by 6 g/kg soil (1.03% humus content), bulk density 1450–1600 kg/m³.

Soil sampling at the field plots. A systematic and non-stratified sampling design using a transect was chosen for this study. This transect has five measurement points to consider different erosion positions from the upper to the lower plot part (Figures 1 and 3). In addition, three reference sites were chosen close to the study site on flat and grassed terrain (Figure 3)
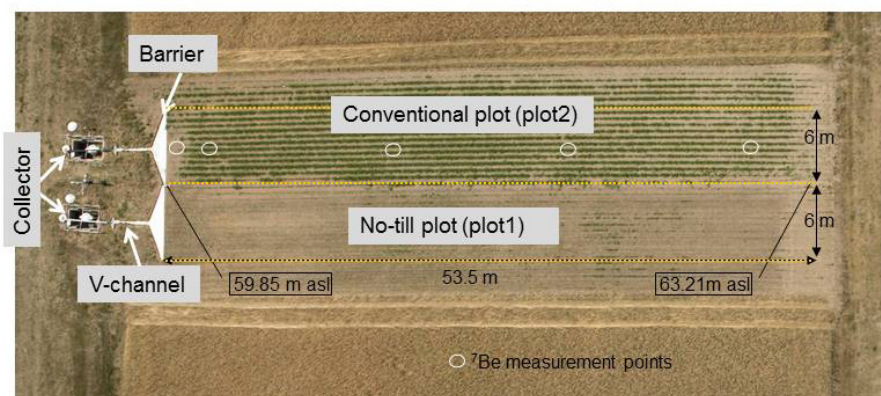

Figure 1. The experimental plots at Müncheberg research station

with no visible evidence for erosion or sedimentation. These were used to derive site-specific data on the undisturbed [7]Be inventory and depth profile.

If the study field was covered with vegetation, plants were taken together with the soil samples and ashed with the soil to acquire total [7]Be inventory at a measurement point. For establishing total inventories of [7]Be at the reference and study points soil samples were taken with a gauge and a scraper plate of 15 cm in length, 20 cm in width and 2 cm in depth. A detailed description of the sampling technique is given in Jha *et al.* (2015).

[7]Be and other measurements. During the study period, 12 short-term erosion events were identified at the tilled plot (Table 1). For the April event (03. 04. 2010), soil redistribution within the study plot was observed, but no soil was collected at the barrier. Soil samples were always taken after heavy rainfall events. Concentrations of [7]Be were measured immediately after sampling by gamma-spectrometry (Jha *et al.* 2015).

In Table 1, the canopy cover of 100% was measured if the plants at the plot (sorghum plants) attained a height of 1.5 m. Rainfall intensities (I_{30}) and rainfall erosivities (EI_{30}) were sufficient for triggering water erosion (Bergsma 2000; Toy *et al.* 2002). These parameters were calculated with the help of algorithms given in USLE or DIN19708 (2005).

Modelling

Water erosion. The erosion simulation of single events and calibration were carried out using the physically based model EROSION-3D (Schmidt 1991, 1996; Schmidt *et al.* 1996; von Werner 1995, 2014). The application of EROSION-3D requires raster-based information on relief, soil and rainfall conditions. Most of these variables are commonly accessible, the model-specific parameters were taken from catalogues or set for best fit with measurements: skin factor, surface roughness and resistance to erosion.

Erosion-3D predicts the spatial and temporal distribution of erosion and deposition as well as the quantity and textural composition of the transported sediment for each raster cell. Some theoretical concepts are presented in Schindewolf and Schmidt (2012). Standard input parameters based on different soil types and cultivation techniques are documented in the parameter catalogue (Michael *et al.* 1996). Laserscan-DEM2 (LGB 2016) model is used as a basis for terrain simulation.

Measured runoff and erosion rates are first compared with the calculated results using the standard values from the parameter catalogue (Michael *et al.* 1996). The parameters were then adjusted by fitting modelled soil loss to the measurements by taking into account the published data as follows:

Table 1. Characteristics of the rainfall and canopy cover for examined erosion events

Erosion event	Date (DD-MM-YYYY)	Canopy cover (%)	Rainfall erosivity (EI_{30}, N/h)[1]	Rainfall intensity (I_{30}, mm/h)[2]	Rainfall depth (P, mm)	Sum of rainfall depth between events (P, mm)
2010						
Apr	03-04-2010	10	1	5	7.9	
May	26-05-2010	100[3]	22	28	32.3	96.6
Jul-1	20-07-2010	30	37	28	59.1	95.6
Jul-2	27-07-2010	50	38	37	52.7	52.7
Aug-1	11-08-2010	100	5	17	15.1	66.7
Aug-2	20-08-2010	100	51	45	50.9	114.7
2011						
June	27-06-2011	5	7	22	12.6	
July	18-07-2011	50	15	29	24.2	75.9
Aug-1	02-08-2011	100	20	12	103.0	152.6
Aug-2	23-08-2011	100	8	22	15.1	17.9
Sep-1	02-09-2011	100	1	7	11.7	30.5
Sep-2	16-09-2011	100	55	59	36.1	67.2
Min		5	1	5	7.9	17.9
Max		100	55	59	103.0	152.6

[1]$EI_{30} = \Sigma(E_i) \times I_{30}$ (N/h); $E_i = (11.89 + 8.73 \log I_i) \times N_i$ (J/m²) for $I_i \geq 0.05$ mm/h; $E_i = 0$ J/m² for $I_i < 0.05$ mm/h; $E_i = 28.33 N_i$ J/m² for $I_i > 76.2$ mm/h; [2]maximal rainfall depth in 30 min; [3]winter catch crop – winter rye

– Surface runoff: calibration of modelled runoff for changing values of skin factors. Skin factors were set so that modelled and measured values of the surface runoff coincided.

– Soil loss: roughness coefficient (s/m$^{1/3}$) and erodibility resistance (N/m^2) are rearranged respectively.

– For each rainfall event erosion/deposition rates estimated by EROSION-3D were compared with the ^{7}Be measurements at the 5 sampling points.

Using the parameters given in Table 2, erosion simulations were carried out for 11 rainfall events as given in Table 1.

^{7}Be model. As depth distributions of ^{7}Be in soils indicate, its convective transport can be neglected. Thus, a 1-D diffusion-sorption model is used for simulating its mobility in soils (Jha *et al.* 2015), which can be written as

$$\frac{\partial C(z,\,t)}{\partial t} = -D \times \frac{\partial^2 C(z,\,t)}{\partial z^2} - \lambda \times C(z,\,t) \qquad (1)$$

where:
$C(z,\,t)$ – concentration of ^{7}Be in soil at depth z (m) and
      time t (s) (Bq/m^3)
D – effective diffusion coefficient (m^2/s)
λ – radioactive decay constant (1/s)

In case of multiple erosion events and when the study plot was ploughed, arbitrary ^{7}Be concentrations

left in soil after each event, analytical solutions of Eq. (1) may be difficult to obtain. Thus, a numerical solution of Eq. (1) has been developed (Jha *et al.* 2015). It is based on a finite difference approximation using the Crank-Nicholson scheme. Simulations of ^{7}Be build-up and relocation in soil are performed until the time of the first erosion event, t_1, at which the total inventory of ^{7}Be, A_1^{num}, is calculated. The erosion rate, Δz_1, is given by the soil depth before erosion where

$$\int_{-\infty}^{\Delta z_1} C^{num}(z,t_1)dz = A_1^{\exp} \qquad (2)$$

where:
$A_1^{\exp}$ – inventory of ^{7}Be just after the erosion event,
      which was determined by soil sampling and
      analysis

RESULTS AND DISCUSSION

Estimation of erosion and deposition rates using the ^{7}Be model. For all erosion events (Table 1), the ^{7}Be technique has been used to estimate soil erosion and deposition rates at the study plot and to compare these with the soil masses collected. Simulations took into account that the ^{7}Be profiles were disturbed by ploughing.

Table 2. Estimated parameters for EROSION-3D model

Erosion event	Skin factor[1]	Roughness[1] (s/m$^{1/3}$)	Erodibility resistance[1] (N/m^2)
2010			
Apr			
May	0.200	0.020	0.00070
Jul-1	0.070	0.013	0.00180
Jul-2	0.050	0.013	0.00100
Aug-1	0.025	0.400	0.00020
Aug-2	0.050	0.400	0.00012
2011			
June	0.020	0.013	0.00100
July	0.001	0.013	0.00030
Aug-1	0.015	0.013	0.00030
Aug-2	0.030	0.013	0.00010
Sep-1	0.130	0.013	0.00030
Sep-2	0.007	0.025	0.00050
Min.	0.001	0.013	0.00010
Max.	0.200	0.400	0.00180
Standard min.[2]	0.03	0.007	0.00007
Standard max.	10	0.4	0.009

[1]Tables 5 and 6 inform about the calibration process to obtain these parameters; [2]standard min., max. in the parameter catalogue

Table 3. Measured soil redistribution at the tilled plot and estimated by the [7]Be method (JHA *et al.* 2015)

Erosion event	Erosion (–)/deposition(+) rates at the measurement points along the slope (kg/m^2)					Soil on the barrier (kg)	
	5 m	20 m	35 m	50 m	53 m	collected	estimated
2010							
Apr	< 0.03	< – 0.006	+ 1.5 ± 0.6	– 0.7 ± 0.6	< 0.02	–	3 ± 3
May	+ 0.5 ± 0.5	+ 0.5 ± 0.5	– 0.6 ± 0.5	+ 1.0 ± 0.6	+ 1.0 ± 0.6	4	0 ± 7
Jul-1	< 0.07	< 0.03	– 1.0 ± 0.5	– 1.0 ± 0.7	< – 0.07	20	22 ± 10
Jul-2	– 0.1 ± 0.5	< – 0.001	+ 0.3 ± 0.5	+ 0.3 ± 1	< – 0.003	24	28 ± 36
Aug-1	< – 0.05	– 0.1 ± 0.5	+ 0.8 ± 0.7	+ 1.8 ± 0.5	– 0.8 ± 0.9	4	16 ± 27
Aug-2	– 0.3 ± 0.5	– 0.6 ± 0.9	– 1.1 ± 0.5	– 1.5 ± 0.5	+ 0.4 ± 0.6	145	124 ± 39
2011							
June	– 0.2 ± 0.9	– 0.2 ± 1.0	< – 0.09	– 0.4 ± 0.5	– 0.2 ± 0.6	16	15 ± 26
July	+ 0.6 ± 0.5	+ 0.7 ± 0.5	+0.2 ± 0.3	+1.3 ± 0.8	– 0.4 ± 0.9	170	16 ± 18
Aug-1	– 1.3 ± 0.8	– 1.6 ± 0.9	– 2.6 ± 0.4	– 0.9 ± 0.9	+ 0.9 ± 0.7	25	9 ± 4
Aug-2	– 0.3 ± 0.5	– 0.5 ± 1.2	< 0.06	– 1.2 ± 1.1	– 0.7 ± 0.5	4	42 ± 27
Sep-1	– 0.2 ± 0.5	< – 0.07	– 0.3 ± 0.8	+ 1.3 ± 0.8	+ 0.7 ± 0.3	13	0 ± 16
Sep-2	– 0.4 ± 1.1	– 0.1 ± 0.8	rill	rill	– 2.4 ± 0.8	161	171 ± 61

Table 3 summarises the simulated soil redistribution rates along the slope. These were used to predict soil accumulation. Results are given together with the soil measured in the sampler system after each erosion event. As discussed by JHA *et al.* (2015), no systematic bias was seen indicating that our methodology is applicable for non-steady state [7]Be inventories, which are common in case of multiple erosion events. The presence of rill erosion and high canopy cover reduces the [7]Be in soil. This results in high measurement uncertainties of [7]Be inventories which are reflected by the erosion rate estimates in Table 3.

The soil erosion and deposition rate estimates along the slope at the tilled plot show the complex redistribution pattern of soil within the study area. This highlights a major advantage of the [7]Be technique over soil sampling at the field bottom: If [7]Be is measured shortly after erosion events at points of interest within an assessment area, detailed information on soil redistribution within the area can be gained with spatial resolution as high as needed.

EROSION-3D modelling results and comparison with [7]Be modelling. After calibration as discussed in section water erosion, surface runoff, erosion rates
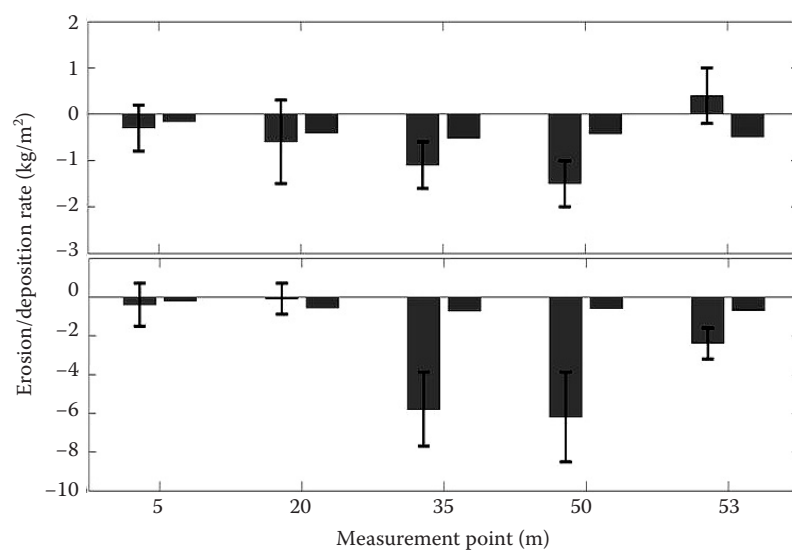

Figure 2. Erosion rates estimated by the [7]Be model (grey bars with uncertainties) and EROSION 3D model (right bars) for Aug-2/2010 (top graph) and Sep-2/2011 (bottom graph) events

and net masses of soil were estimated with the help of EROSION-3D.

The skin factors were event-wise adjusted as the infiltration conditions became very dynamic (Tables 2 and 5). Due to the large siltation and soil-crusting affinity of the silty sand, estimates of the skin factors were between 0.001 and 0.2. For the larger events the smallest values were applied (Table 2). Soil erodibility was greatest during these events (rills and sealed/crusted soil surface). The erodibility values for all events are between 0.0001 and 0.0018, which corresponds to the data range listed in the parameter catalogue (Table 2). The September-2-2011 event with a four-times higher erosivity value shows the effect of the nearly 100% soil cover compared to the July 2011 event with a similar soil loss (Table 1, 3 and 4). Figure 2 shows the erosion rates estimated for two events. The deposition rate estimated for the August-2 event (Figure 2 top) at 53 m reflects the "residue" sedimentation caused by the proximity of this sampling point to the sampler system.

The parameter values given in Table 2 were adjusted until the best fit between modelled and measured soil was obtained. Therefore during all 11 events a very good agreement between modelled and measured soil can be seen (Table 4).

Table 3 shows that during the August-2-2010 event heavy erosion occurred when a sheet of soil was deposited between the measurement point at 53 m and the sampler system. A soil layer of 15 cm in thickness was collected after this event. EROSION-3D results in Table 4 show a high erosion rate instead of depo-

sition at 53 m. This is because the model does not take into consideration the presence of the sampler system. In this case due to the combination of measurement and modelling, the ^{7}Be method provides a better result. The depositions caused by the barrier effect of the installed measuring equipment can be detected by the ^{7}Be method.

As represented in Table 1, during the Sept-2 event in 2011, a full canopy cover was developed. Despite this heavy vegetation cover, during this event 161 kg of soil were collected. For events with higher rain intensities the interception of plants decreases and the share of throughfall increases (von Hoyningen-Huene 1983; Toy *et al.* 2002). This combined with water falling from the leaves creates high runoff velocities which lead to surface, rill and interrill erosion (Toy *et al.* 2002). During this event rills were observed mainly at 35–50 m (Jha *et al.* 2015). The ^{7}Be and EROSION-3D models both estimate very high erosion rates during this event (Table 3). Figure 3 depicts the spatial distribution of the sediment budget for the Sept-2 event in which 161 kg soil loss was measured. Dark orange colours here denote the high erosion rates for this event. The soil loss modelled by EROSION-3D given in Table 4 fits well with the estimate of the ^{7}Be methodology (Table 3). Compared to the adjacent slope areas, less soil erosion (light orange) is the result of the reduced slope length shortened by this barrier, which causes a lower transport capacity of the flowing suspension. A similar soil loss to the neighbouring areas (in dark red) is achieved only on the lower slope, after about

Table 4. Modelled and measured soil erosion at the conventional tilled plot by EROSION-3D

Erosion event	Erosion rates at the measurement points along the slope (kg/m^2)					Soil on the barrier (kg)	
	5 m	20 m	35 m	50 m	53 m	collected	modelled
2010							
May	0.003	0.013	0.017	0.014	0.016	4.0	3.7
Jul-1	0.026	0.071	0.090	0.070	0.076	20.0	19.5
Jul-2	0.033	0.088	0.113	0.090	0.100	24.0	25.0
Aug-1	0.000	0.016	0.023	0.017	0.013	4.0	4.3
Aug-2	0.155	0.405	0.522	0.420	0.483	145.0	116.0
2011							
June	0.032	0.078	0.098	0.077	0.056	16.0	16.0
July	0.298	0.795	1.025	0.821	0.943	170.0	158.0
Aug-1	0.014	0.068	0.089	0.069	0.082	25.0	67.0
Aug-2	0.003	0.011	0.015	0.012	0.014	4.0	3.2
Sep-1	0.017	0.048	0.061	0.049	0.057	13.3	13.5
Sep-2	0.208	0.545	0.715	0.576	0.677	161.0	158.0

Table 5. Runoff calibration for the soil (Su2), examples for 4 events

Erosion event	Bulk density (kg/m^3)	C$_{org}$ (%)	SKIN factor	Initial moisture (%)	Surface runoff		
					measured	modelled	modelled to measured
					(l)		
2010							
	1 600	0.6	0.1	25	4 030	2 370	0.6
Jul-1	1 600	0.6	0.02	25	4 030	8 020	2.0
	1 600	*0.6*	*0.07*	*25*	*4 030*	*4 040*	*1.0*
Jul-2	1 600	0.6	0.07	25	2 580	1 580	0.6
	1 600	*0.6*	*0.05*	*25*	*2 580*	*2 320*	*0.9*
	1 600	0.6	0.07	25	1 360	69	0.1
Aug-1	1 600	0.6	0.05	25	1 360	330	0.2
	1 600	*0.6*	*0.025*	*25*	*1 360*	*1 280*	*0.9*
2011							
	1 600	0.6	0.07	25	7 760	8 150	1.1
Sep-2	1 600	0.6	0.13	25	7 760	4 350	0.6
	1 600	*0.6*	*0.007*	*25*	*7 760*	*7 320*	*0.9*

In italics – used values in modelling

60 m of the slope length. Since the plots are situated on a straight slope, no sedimentation/accumulation/colluviation take place. This is not in contradiction with the above-mentioned fact that sedimentation is caused by the barrier at the bottom plot.

EROSION-3D has been developed mainly for the agricultural advisory services, which involves understanding and integrating the main processes leading to water erosion. Thus EROSION-3D has provided a variety of protective measures. If no measurements of soil erosion and surface runoff exist, generic parameter values are used. Table 5 shows calibrated input data for the purpose of reproducing measured runoff and soil erosion values. As an example, the default skin parameter is set to 1. Sealing, crusting and soil compaction reduce the infiltration of rain-
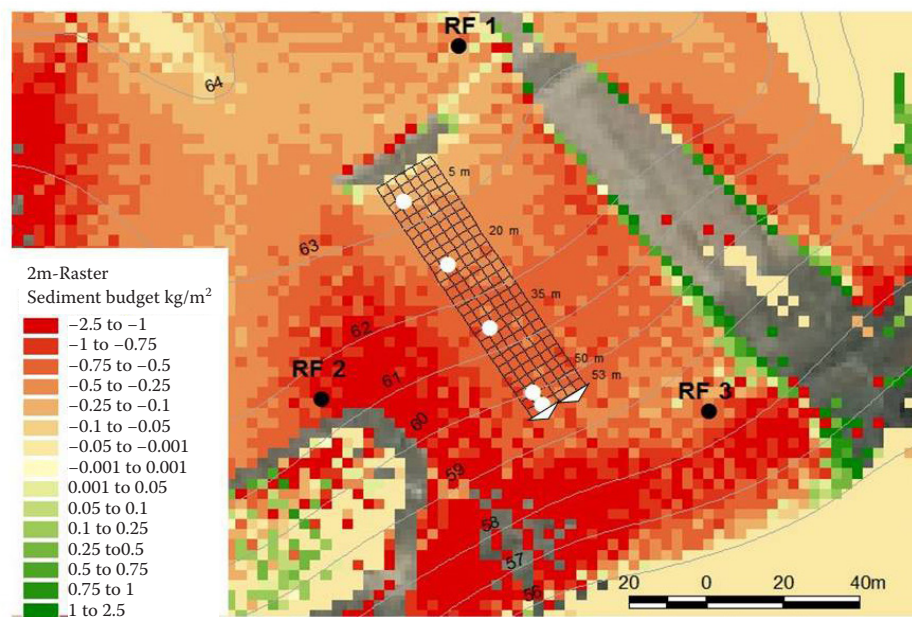

Figure 3. Result of EROSION-3D for Sep-2/2011: erosion (–) – deposition (+) on the plots (conventional management on the whole area) and sampling design for [7]Be measurements (white points and RF – reference sites)

Table 6. Calibration of soil parameters influencing soil loss (erosion event Jul-1/2010)

Roughness (s/m$^{1/3}$)	Erodibility (N/m^2)	Soil loss		modelled to measured
		measured	modelled	
		(t/ha)		
0.013	0.00020	0.616	5.608	9.1
0.013	0.00200	0.616	0.543	0.9
0.013	0.00150	0.616	0.732	1.2
0.013	*0.00180*	*0.616*	*0.606*	*1.0*

In italics – used values in modelling

water into the soil and thus the parameter values must be set < 0. Similarly, roughness, erodibility and crop cover were adjusted as illustrated in Table 6 for the July-1 event.

From Tables 3 and 4 it can be concluded that there generally exists a good agreement between the two erosion estimation techniques. The EROSION-3D model considers more dynamic factors such as vegetation cover and soil roughness, thereby modelling an accurate soil loss for all events. In our study EROSION-3D had to be calibrated by adjusting its various parameters to the soil observed – a procedure presently inevitable due to its limited parameter data base which had been mainly derived from irrigation experiments (Michael *et al.* 1996). However, our results offer the potential of using [7]Be derived erosion rates for improving this data base. In contrast to installing barriers at the slope bottom, this approach will allow to include also within-plot soil relocation rates.

CONCLUSIONS

The results presented in this paper show that both the [7]Be technique and after calibration EROSION-3D give consistent estimates of eroded soil masses at our study plot and contribute to our understanding of the dynamics and processes of soil erosion by water. From the quantitative analysis provided here the following conclusions can be made:
– The EROSION-3D model estimates erosion rates within the study plot. For this purpose measured soil data within the study plot is not either documented or used. Instead, the erosion rates were estimated with the use of physically based equations for the texture-specific transport capacity.
– Process-based modelling combined with the [7]Be technique and actual soil measurements can be highly recommended for improving event-based erosion modelling.
– The plot internal erosion and deposition rates estimated by our [7]Be-methodology assist in understanding soil relocation processes at our study site and in quantifying them.
– Additional erosion studies are needed to fully explore the potentials of both the [7]Be techniques and process-based models such as EROSION-3D for erosion assessments.
– Modern techniques such as laser scan measurements should offer the potential to get observational data on soil dislocation by erosional events (Schneider *et al.* 2013, Deumlich *et al.* 2014), which may be welcome for further validating the [7]Be technique and EROSION-3D simulations.

References

AG Boden (2005): AG Boden der Staatlichen Geologischen Dienste und der Bundesanstalt für Geowissenschaften und Rohstoffe. Bodenkundliche Kartieranleitung [Soil mapping] 5. Auflage (KA5). Stuttgart, Hannover, Schweizerbart'sche Verlagsbuchhandlung, (as KA5 cited). (in German)

Bergsma E. (2000): Terminology for Soil Erosion and Conservation. Wageningen, International Society of Soil Science (ISSS).

Blake W., Walling D.E., He Q. (1999): Fallout [7]Be as a tracer in soil erosion investigations. Applied Radiation and Isotopes, 51: 599–605.

Deumlich D., Dannowski R., Völker L. (2014): Historical and actual geoinformation – basis for agricultural landscape research. Zeitschrift für Geodäsie, Geoinformation und Landmanagement, 139: 329–341. (in German)

Govers G., Quine T.A., Desmet P.J.J., Walling D.E. (1996): The relative contribution of soil tillage and overland flow erosion to soil redistribution on agricultural land. Earth Surface Processes Landforms, 21: 929–946.

Hjulström F. (1935): Studies of the morphological activity of rivers as illustrated by the River Fyris. Bulletin of the Geological Institute University of Uppsala, 25: 221–527.

Jha A., Schkade U., Kirchner G. (2015): Estimating short-term soil erosion rates after single and multiple rainfall

events by modelling the vertical distribution of cosmogenic [7]Be in soils. Geoderma, 243–244: 149–156.

LGB (2016): https://www.geobasis-bb.de/geodaten/dgm-laserscan.htm

Malam Issa O., Le Bissonnais Y., Planchon O., Favis-Mortlock D., Silvera N., Wainwright J. (2006): Soil detachment and transport on field- and laboratory-scale interrill areas: erosion processes and the size-selectivity of eroded sediment. Earth Surface Processes and Landforms, 31: 929–939.

Matisoff G., Bonniwell E.C., Whiting P.J. (2002): Soil erosion water sources in Ohio watershed using Be-7, Cs-137 and Pb-210. Journal of Environmental Quality, 31: 54–61.

Meyer L.D., Foster G.R., Romkens M.J.M. (1975): Mathematical Simulation of Upland Erosion Using Fundamental Erosion Mechanics. In: Proc. Sediment Yield Workshop, Oxford, USDA Sedimentation Laboratory: 177–189.

Michael A., Schmidt J., Schmidt W.A. (1996): Erosion 2D/3D – a Computer Model to Simulate Water Erosion – Parameter Catalogue. Freistaat Sachsen, LfL, LfUG, Freiberg. (in German)

Oldeman L.R. (1994): The global extent of soil degradation. In: Greenland D.J., Szabolcs I. (eds): Soil Resilience and Sustainable Land Use. Wallingford, CAB International: 99–118.

Olsen C.R., Larsen I.L., Lowry P.D., Cutshall N.H., Todd J.F., Wong G.T.F., Casey W.H. (1985): Atmospheric fluxes and march-soil inventories of [7]Be and [210]Pb. Journal of Geophysical Research, 90: 10487–10495.

Porto P., Walling D.E. (2014): Use of [7]Be measurements to estimate rates of soil loss from cultivated land: Testing a new approach applicable to individual storm events occurring during an extended period. Water Resources Research, 50: 8300–8313.

Ritchie J.C., Ritchie C.A. (2007): Bibliography of publications of ^{137}Cs studies related to on and sediment deposition. Avaiable at www.ars.usda.gov/Main/docs.htm?docid=15237

Rodenas C., Gomez J., Quindos L.S., Fernandez P.L. (1997): [7]Be concentrations in the air, rain water and soil in Cantabria (Spain). Applied Radiation and Isotopes, 48: 545–548.

Rosner G., Hötzl H., Winkler R. (1996): Continues wet-only and dry-only deposition measurements of ^{137}Cs and [7]Be: an indicator of their origin. Applied Radiation and Isotopes, 47: 1135–1139.

Schindewolf M., Schmidt J. (2012): Parameterization of the EROSION 2D/3D soil erosion model using a small-scale rainfall simulator and upstream runoff simulation. Catena, 91: 47–55.

Schmidt J. (1991): A mathematical model to simulate rainfall erosion. Catena, 19: 101–109.

Schmidt J. (1996): Development and use of a physical based simulation model for the erosion of inclined agricultural used fields. Berliner Geographische Abhandlungen, 61: 148. (in German)

Schmidt J., v. Werner M., Michael A. (1996): Erosion 2D/3D – a computer model to simulate water erosion. Dresden, Sächsische Landesanstalt für Landwirtschaft. (in German)

Schneider A., Gerke H.H., Maurer T., Nenov R. (2013): Initial hydro-geomorphic development and rill network evolution in an artificial catchment. Earth Surface Processes and Landforms, 38: 1496–1512.

Schuller P., Walling D.E., Sepulveda A., Trumper R.E., Rouanet J.L., Pino I., Castillo A. (2004): Use of ^{137}Cs measurements to estimate changes in soil erosion rates associated with changes in soil management practices on cultivated land. Applied Radiation Isotopes, 60: 759–766.

Schuller P., Iroume A., Walling D., Manchilla B.H., Castillo A., Trumper E.R. (2006): Use of Beryllium-7 to document soil redistribution following forest harvest operations. Journal of Environmental Quality, 35: 1756–1763.

Schuller P., Sepulveda A., Castillo A., Walling D. (2008): Use of [7]Be to document soil erosion associated with a short period of extreme rainfall. Journal of Environmental Radioactivity, 99: 35–49.

Sommer M., Gerke H.H., Deumlich D. (2008): Modelling soil landscape genesis - A "time split" approach for hummocky agricultural landscapes. Geoderma, 145: 480–493.

Tilley D.R., Cheves C.M., Godwin J.L., Hale G.M., Hofmann H.M., Kelley J.H., Sheu C.G., Weller H.R. (2002): Energy levels of light nuclei A = 5, 6, 7. Nuclear Physics A, 708: 3–163.

Toy T.J., Foster G.R., Renard K.G. (2002): Soil Erosion: Processes, Prediction, Measurement and Control. New York, John Wiley & Sons, Inc.

von Hoyningen-Huene J. (1983): Influence of land use on landscape water houshold. Part I: Interception of Rainfall in Agricultural Crops. DVWK-Schriften 57, Hamburg, Berlin, Verlag Paul Parey: 1–51. (in German)

Von Werner M. (1995): GIS-oriented methods for the relief analysis to model soil erosion in small watersheds. [Ph.D. Thesis.] Berlin, Freie Universität Berlin. (in German)

Von Werner M. (2014):. http://www.bodenerosion.com/demos/e3d300/SampleProject.pdf

Wallbrink P.J., Murray A.S. (1993): Use of fallout radionuclides as indicators of erosion processes. Hydrological Processes 7: 297–304. Wallbrink P.J., Murray A.S. (1996): Distribution and variability of [7]Be in soils under different surface cover conditions and its potential for describing soil redistribution processes. Water Resources Research, 32: 467–476.

Walling D.E., Bradley S.B. (1988): The use of caesium-137 measurements to investigate sediment delivery from cultivated areas in Devon, UK. IAHS Publ. No. 174: 325–335.

Walling D.E., Woodward J.C. (1992): Use of radiometric fingerprints to derive information on suspended sediment sources. In: Erosion and Sediment Transport Monitoring Programmes in River Basins. IAHS Publ. No. 210: 153–164.

Walling D.E., Quine T.A. (1995): The use of fallout radionuclide measurements in soil erosion investigations. In: Proc. Int. Symp. Nuclear Techniques in Soil-plant Studies for Sustainable Agriculture and Environment Preservation, Vienna, Oct 1994. Vienna, IAEA Proceeding Series STI/PUB/947: 597–619.

Walling D.E., He Q., Blake W. (1999): Use of ^{7}Be and ^{137}Cs measurements to document short- and medium-term rates of water induced soil erosion on agricultural land. Water Resources Research, 35: 3865–3874.

Wilson C.G., Matisoff G., Whiting P.J. (2003): Short-term erosion rates a 7Be inventory balance. Earth surface Processes and Landforms, 28: 967–977.

Wischmeier W.H., Smith D.D. (1978): Predicting Rainfall Erosion Losses – A Guide to Conservation Planning. USDA Agriculture Handbook No. 537. Washington D.C., USDA.

Young R.A., Onstad C.A. (1976): Predicting particle size composition of eroded soil. Transactions of the ASAE, 19: 1071–1075.

Zapata P. (2002): Handbook of Assessment of Soil Erosion and Sedimentation Using Environmental Radionuclides. London, Kluwer Academic Publishers.

Zapata F. (2003): Field application of the Cs-137 technique in soil erosion and sedimentation. Soil and Tillage Research, 69 (Special Issue): 1–153.

Zapata F. (2007): Use of environmental radionuclides to monitor soil erosion and sedimentation in the field, landscape and catchment level before, during and after implementation of soil conservation measures. Science Publishers: 301-317.